

Received:

4 June 2017

Revised:

17 December 2017

Accepted:

8 February 2018

Cite as: Ramadan Abdelaziz,
Yasser Abd El-Rahman,
Sophie Wilhelm. Landsat-8
data for chromite prospecting
in the Logar Massif,
Afghanistan.
Heliyon 4 (2018) e00542.
doi: [10.1016/j.heliyon.2018.e00542](https://doi.org/10.1016/j.heliyon.2018.e00542)



Landsat-8 data for chromite prospecting in the Logar Massif, Afghanistan

Ramadan Abdelaziz ^{a,c,*}, Yasser Abd El-Rahman ^b, Sophie Wilhelm ^c

^a College of Engineering, A'Sharqiyah University, Oman

^b Geology Department, Cairo University, Giza 12613, Egypt

^c TU Bergakademie Freiberg, Freiberg, Germany

* Corresponding author.

E-mail addresses: ramawaad@gmail.com, ramadan.abdelaziz@asu.edu.om (R. Abdelaziz).

Abstract

Chromite is widely distributed in the east and southeast of Afghanistan, especially in Logar Province. Chromite mineralization is podiform-type and is hosted in the stratigraphically lowest ultramafic rocks of the Logar Ophiolite Complex. This ophiolite complex represents a remnant of an early Cretaceous oceanic crust that was thrusted over a late Permian to Mid-Jurassic platform-type sequence of the Kabul Terrane during the Himalayan Orogeny. The ultramafic rocks are composed mainly of dunite and harzburgite, which are variably serpentinized. Chromite mineralization of the Logar area ranges from massive chromitite pods to disseminated chromite crystals in the ultramafic rocks. Microscopically, the chromite exhibits granular texture and is generally fresh; however, some magnetite and/or ferrichromite are formed along the fractures of some chromite grains. The primary interstitial silicate minerals of the massive chromite and the silicate minerals surrounding the disseminated chromite grains are completely altered to serpentine along with some chlorite. Thus, serpentinite is most likely the host of the chromite in the Logar Province. The main aim of this study is discriminate serpentine using the Landsat 8 Operational Land Imager (OLI). The serpentinite of the Logar Province is separated by the combination of bands, principal components, band ratios, and supervised classification techniques. Using Landsat 8 and supervised classification with maximum likelihood

classification as a tool for mineral exploration improve lithological mapping in the Logar Valley area.

Keywords: Geochemistry, Geology, Earth sciences

1. Introduction

The ultramafic sections of ophiolitic sequences host a significant amount of podiform chromitite bodies (Paktunc, 1990; Rollinson, 2005; Ahmed et al., 2009; Miura et al., 2012). These ultramafic rocks commonly exhibit a variable degree of serpentinization (Abu El Ela and Farahat, 2010; González-Jiménez et al., 2011; Grieco and Merlini, 2012; Ahmed, 2013). Mapping these serpentinized areas using remote sensing is the most appropriate technique in arid regions that have no vegetation cover (Gad and Kusky, 2006; Amer et al., 2010; Rajendran et al., 2012; Pournamdari et al., 2014a, b). Moreover, remote sensing is an important tool to map areas with rough topography or areas, which are difficult to access due to political problems.

Chromitite is widely distributed in Afghanistan, especially in the east and southeast parts of the country. It occurs in Logar, Kabul, Kandahar, Khost, Paktia, Nangarhar, Parwan, and Vadak Provinces (Orris and Bliss, 2002). Among these locations, the chromite deposits of the Logar Valley ophiolitic complex are the most studied ones. The Logar Valley area is located 33 km south of Kabul and extends between latitudes 34° 05' to 34° 25' North and longitudes 68° 45' to 69° 10' East. It has a total resource of, at least, 181,000 tons (Volin, 1974).

The main aim of the study is to discriminate the lithological and hydrothermal alteration of the different rock units in the Logar valley area, especially the serpentine units, which encloses the chromite lenses. For lithological mapping and discrimination between the different rock units, remote sensing is the most suitable tool to be applied in Afghanistan locations that are classified as arid terrane. An image subset of Landsat 8 OLI data (153/36 path/row, acquisition date 27/12/2014) has been processed using the ERDAS IMAGINE (Earth Resource Data Analysis System) processing and ArcGIS (geographic information system) software. The satellite images were projected in the UTM Zone N42 and WGS 1984 ellipsoid (oblate spheroid) datum. The satellite images processing techniques such as false color composites (FCC), principal components analysis (PCA), and band rationing were applied to achieve the main purpose of the study.

2. Geological setting

Afghanistan is located at the western end of the Himalayan mountain range. Such location explains its complicated and long tectonic history. It is composed of a series

of discrete tectonic blocks, which resulted from the successive accretion of Gondwana fragments to the active margin of Laurasia. The accretion events initiated during the Paleozoic Era and had terminated by the closure of the Tethys Ocean and the collision of Laurasia with Gondwana in late Cretaceous-early Paleogene time (Tappognier et al., 1981). These blocks are separated by fault zones. Tectonically, Afghanistan is divided into the northern Afghan-Tajik platform, which is a part of the Laurasian plate and the southeast Katawaz basin, which is the northwestern extension of the India plate. These two units are separated by the Central Afghanistan Terrane along with Kabul and Nuristan Terranes (Fig. 1a).

The eastern side of the Logar area is covered by the Argandab-Helmand block (Fig. 1b), which represents the western extension of the Central Afghanistan terrane. This block is composed mainly of early to middle Proterozoic schists and gneisses (Shareq et al., 1980) that were identified by Livo and Johnson (2011) as the Pagham metasedimentary rocks (Fig. 1c). The Argandab-Helmand block is separated from the Kabul terrane by the Chapman strike-slip fault (Faryad et al., 2015). The Kabul terrane is composed mostly of Neoarchean-Proterozoic basement and a Phanerozoic platform-type carbonate sequence (Faryad et al., 2015). Following the tectono-stratigraphic division compiled by Bohannon (2010) for the Kabul terrane, the Proterozoic basement constitutes the older Sherdarwaza orthogneiss and migmatite, which is overlain by metaquartzite, schists, gneisses and amphibolites of the Kharog Formation. The latter is conformably overlain by the late Proterozoic Welayati Formation, which is composed of amphibolite and schist. The Neoarchean-Proterozoic basement is overlain commonly by the Permian to Jurassic alternating carbonate sequence with minor clastic rocks of the Khengil Series (Fig. 1c). The Neogene (Miocene-Pliocene) basin-fill and fan deposits of the Lataband Series is exposed in the Logar area and are overlain, along with the other units by the Pleistocene to Holocene alluvium (Fig. 1c). These surficial deposits include fine-grained wind-blown sediments, landslide masses and agriculturally altered terrains.

The Logar ophiolite massif represents a fragment of the Mesozoic oceanic crust that was obducted on the Kabul terrane during the Himalayan orogeny. The ophiolite complex is overlain by a volcano-sedimentary sequence and accretionary prism sediments of Cretaceous age (Benham et al., 2009). The Logar ophiolite massif is separated from the Argandab-Helmand block to the west by steeply dipping N-S trending Chapman Fault. To the east, there is the Altimur Fault and Shareq et al. (1980) set the Abparan Thrust, which separates the autochthonous Kabul terrane from the obducted Logar ophiolitic rocks.

The Logar ophiolite is divided structurally and lithostratigraphically into lower ultramafic rocks, which grade upward to the gabbro and central dolerite zone and finally to pillow lavas and associated sedimentary rocks (Benham et al., 2009). The ultramafic rocks constitute the main part of the Logar ophiolite (Fig. 1d) with about

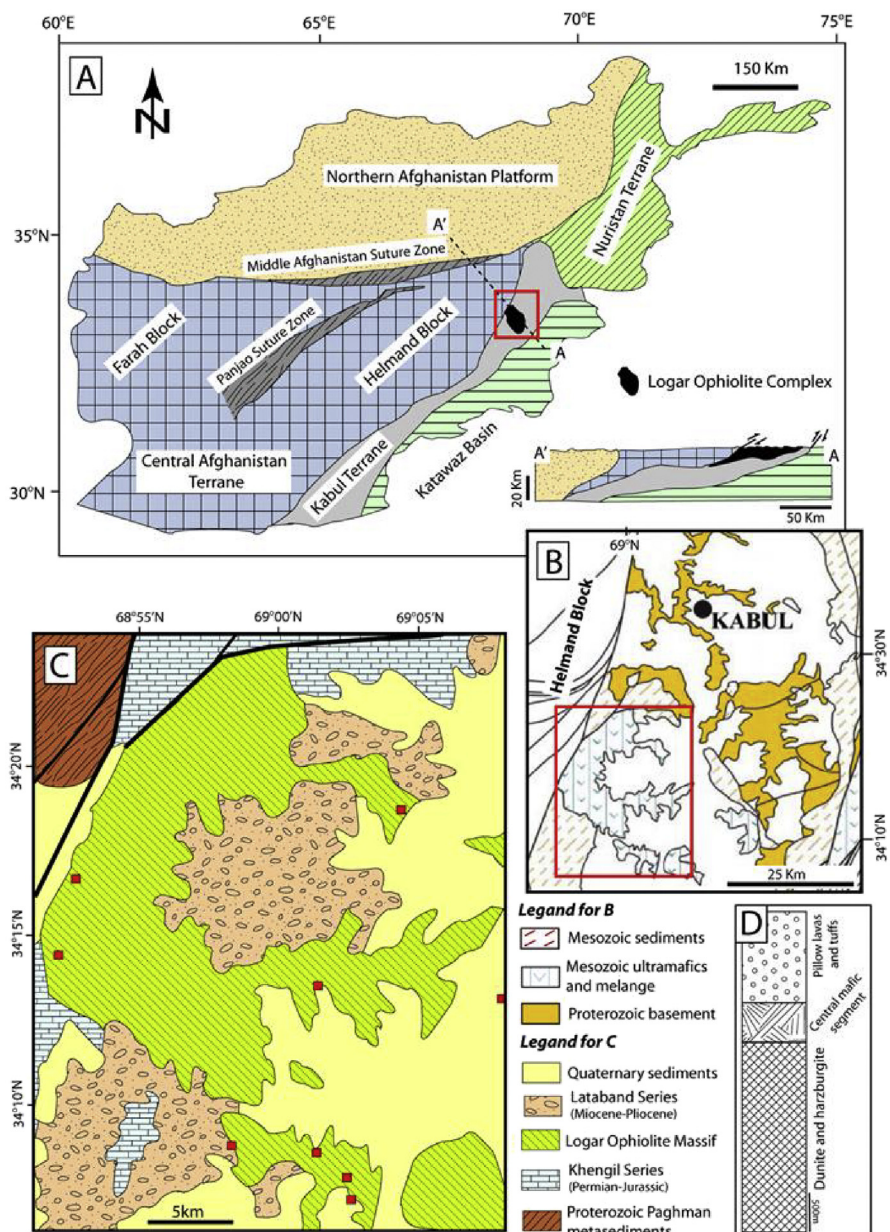


Fig. 1. (A) A simplified geologic map of Afghanistan (after Benham et al., 2009 and Collet et al., 2015). (B) Simplified geological map of the central part of the Kabul terrane outlined as red square in A (Kafarsky et al., 1975). (C) Geological map of the Logar Ophiolite outlined as red rectangle in B (Dronov et al., 1972); the locations of the chromitite occurrences are marked as red solid squares. (D) Simplified litho-stratigraphic section of the Logar ophiolite (modified after Benham et al., 2009).

2800 m of thickness, and are composed mainly of harzburgite and dunite with minor lherzolite and wehrlite. These rocks are variably brecciated and serpentized. The ultramafic rocks grade upward to the central mafic segment of the Logar ophiolite. This segment is composed of a pyroxenite-layered gabbro zone and dolerite dikes complex. The dolerite dikes dip steeply and are 1–15 m thick. Some of these dikes

are traceable for up to 5 km (Benham et al., 2009). The uppermost part of the Logar ophiolite is represented by a 1800 m thick sequence of pillow lavas and associated breccias and tuffs. These basic rocks are comprised of basalt, andesite and spilite, which show either aphyric or porphyritic texture. Nevretdinov and Mirzamon (1979) assigned late Cretaceous age for the dating of both the dolerite dikes and to the andesitic basalt from the Logar ophiolite. The formation of the Logar ophiolite was complex as the tectonic setting of origin of this ophiolite evolved from a mid-ocean ridge to supra-subduction zone setting (Benham et al., 2009).

Chromitite occurs as irregular- and lenticular-shaped massive bodies hosted in the harzburgite and dunite of the Logar ophiolite. This rock assemblage is reminiscent to the transitional zone at the upper portion of the ophiolitic sequences mantle rocks (e.g., Paktunc, 1990; Arai, 1997). The contact between the chromitite and the ultramafic rocks is commonly sharp. The dunite and the harzburgite enclosing the chromitite are intensively serpentized (Fig. 2a). The former shows a mesh texture due to the serpentization of olivine, which exhibit a primary adcumulate texture, while the latter shows bastite texture due to pseudomorphic alteration of orthopyroxene.

Chromite constitutes >90 percent volume of the massive chromitite of the Logar ophiolite and it exhibits allotriomorphic granular texture. Interstitial silicate minerals are completely altered to serpentine and chlorite in order of decreasing abundance. Chromite crystals show no sign of intense alteration and so exhibit dark red to reddish brown color (Fig. 2a). Alteration is limited to minor fractures along which the color darkens due to the alteration of chromite with ferrit-chromite and magnetite (Fig. 2b). Platinum-group minerals are recorded in the chromitite and associated serpentized dunite of the Logar ophiolite by Benham et al. (2009).

3. Results

3.1. False color composites and principal component analysis

Lithological mapping of the Logar Valley area was generated using Landsat 8 OLI (Operational Land Imager). The Landsat-8 OLI image of the study area was processed with ERDAS IMAGINE and ArcGIS software. The Landsat 8 OLI and the Thermal Infrared Sensor (TIRS) were launched in February 2013 by NASA. It contains eight spectral bands (1–7 and 9) with spatial resolution of 30 m, two thermal bands 10 (10.60–11.19 μm) and 11 (11.50–12.51 μm) with 100 m spatial resolution, while the spatial resolution for panchromatic band 8 (0.50–0.68 μm) is 15 m. Band 1 (0.43–0.45 μm) is used for coastal studies, while band 9 (1.36–1.38 μm) is used for cirrus cloud detection. Bands 10 and 11 are used to detect surface temperatures. The Landsat 8 OLI considered for the present study was acquired on 27th December 2014 and provided by NASA. The study area is located in a continental climate; there is a lack of rain and the area is also dry.

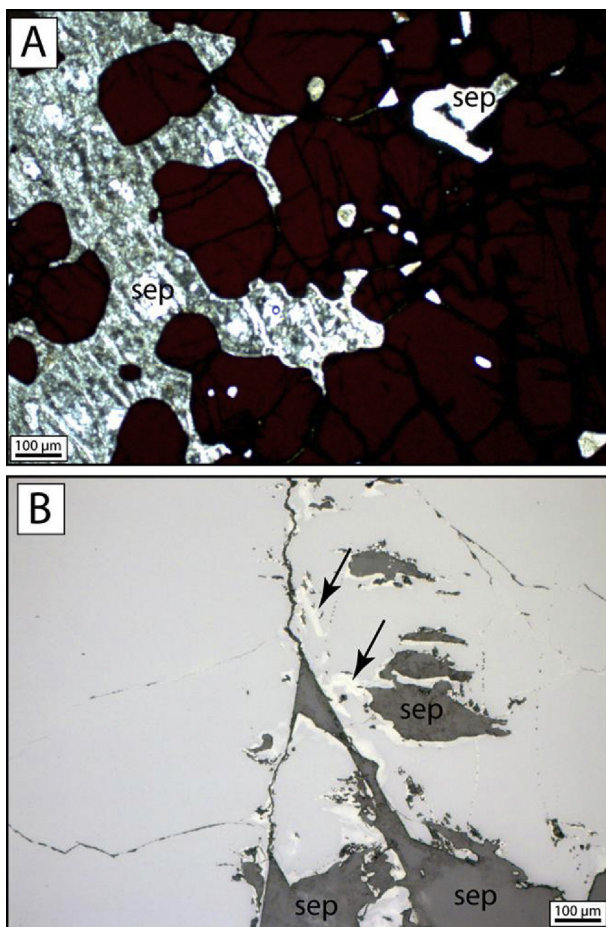


Fig. 2. Photomicrographs of the Logar chromitite. (A) Fresh reddish brown granular chromite embedded in serpentine (sep) showing bastite texture. (B) Chromite altered along the cracks into magnetite showing higher reflectance (black arrows).

To identify the serpentized ultramafic rocks enclosing the chromite lenses from the surrounding rocks units in the Logar Valley area, different analytical techniques were used, including FCC, PCA, and band-ratio images. The false color composite band 2 (Blue), band 5 (NIR), and band 7 (SWIR-2) have been used, where the wave lengths for bands in Landsat 8 OLI are 0.45–0.51 μm, 0.85–0.88 μm, and 2.11–2.29 μm, respectively. This combination provides the highest variance and the least correlation. Fig. 3a shows the false color composite which is generated from bands 752 in RGB. This composite of bands shows the ophiolitic rocks in variable shaded brown color. The Paghman metasedimentary rocks to the northwest side of the Logar ophiolitic rocks are distinguished by light buff and pink colors, while the Khengil carbonate is characterized by gray-blue color in the southern and northern parts of the area. The Neogene and Quaternary deposits constitute the low relief area relative to the three other rock units.

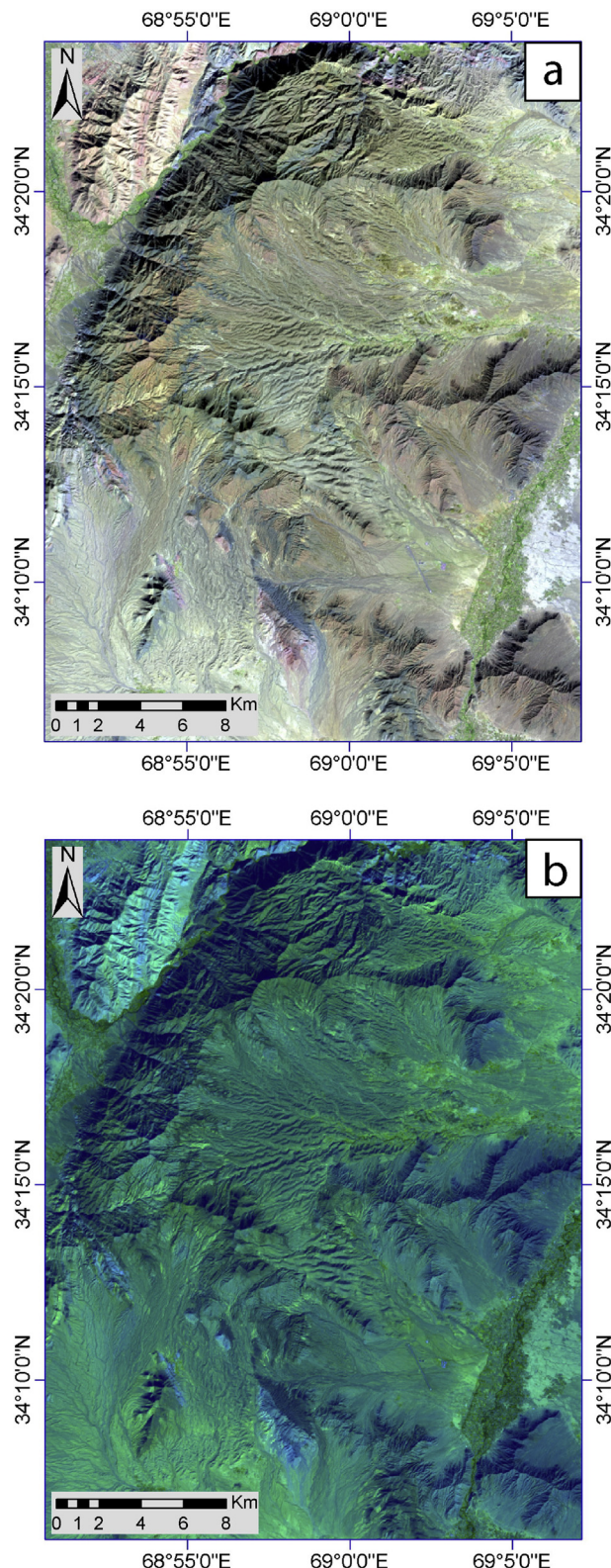


Fig. 3. (A) Landsat8 false color composite image (R:7, G:5, and B:2) in Logar Valley. (B) Landsat8 OLI Principal Component analysis in Logar Valley.

PCA provides the best discrimination between the rocks units to construct a geological map for the Logar Valley area. It is also a useful statistical tool that is used in the field of remote sensing for image compression (Pournamdari et al., 2014a, b), where the PCA assembles a big set of data into a few bands, which reduces the number of dimensions and transforms the correlated set of data into uncorrelated data. The PCA is a linear combination of the original image bands. The first three components (PC 1, PC 2, and PC 3) represent the domain variation in the dataset and highlight the most common feature for all bands (Fig. 3b). The schist and gneiss of the Paghman metasedimentary rocks are distinguished from the ophiolitic rocks and the Khengil carbonate by their light green-blue color.

3.2. Band ratio color composite images

Using band ratios is another technique to divide a measure of reflectance for the pixels in one image band by the measure of reflectance for the pixels in another image band. In other words, a band ratio is a technique through which the digital number value of one band is divided by that of another band. The band ratios technique is used to minimize shadow effects, especially in mountainous areas, which is one of the major problems in satellite imaging (Shahtahmassebi et al., 2013). Band ratios are useful also in highlighting certain features or materials that cannot be seen in raw bands. Different band ratio images (7/6, 6/5, 4/2), (6/4, 6/2, 7/6), and (6/7, 6/5, 4/2) are used for mapping the Logar ophiolite by discriminating between the serpentinized ultramafic rocks and the surrounding various sedimentary rock types (Fig. 4a, b, c).

In the band ratio images (7/6, 6/5, 4/2) and (6/7, 6/5, 4/2) in RGB (Fig. 4a, c), the Logar ophiolite is distinguished by a medium buff-green color, while in the band ratio image (6/4, 6/2, 7/6) in RGB (Fig. 4b), the ophiolitic rocks appear as medium

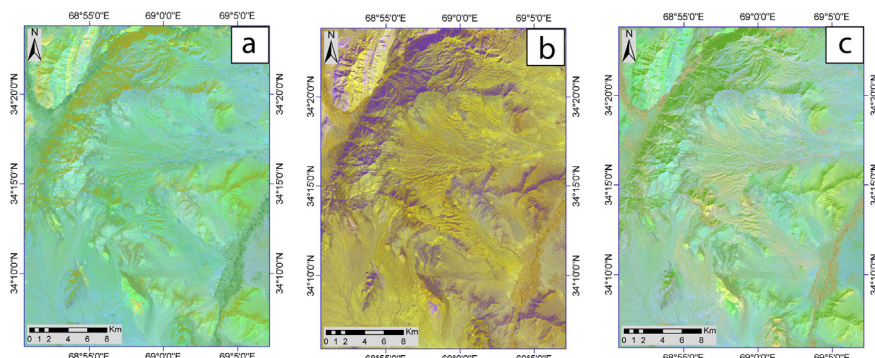


Fig. 4. Landsat8 OLI band ratio color image: (A) (7/6, 6/5, 4/2), (B) (6/4, 6/2, 7/6), and (C) (6/7, 6/5, 4/2) in Logar Valley.

purple-yellow color ([Fig. 4b](#)). The Paghman metasedimentary unit to the northwest of the Logar Valley area appears paler in tones relative to the ophiolitic rocks in the first two band ratios ([Fig. 4a, c](#)), while in [Fig. 4b](#), it appears as a rosy-yellow color. However, it is difficult to distinguish between the ophiolitic rocks and the Khengil series with the band ratio images (7/6, 6/5, 4/2), (6/4, 6/2, 7/6), and (6/7, 6/5, 4/2) in RGB. The Neogene and Quaternary deposits are characterized by a more bluish shade relative to the other rocks units in the band ratio image (7/6, 6/5, 4/2) and exhibits parallel to dendritic drainage patterns ([Fig. 4a](#)). Vegetation along the Logar Valley to the southeast is distinguished as brown ([Fig. 4c](#)) in the band ratio image (6/7, 6/5, 4/2).

The Logar ophiolite is composed mainly of ultramafic rocks and serpentinization is commonly produced from the hydrothermal alteration of olivine and pyroxenes of these rocks ([Fig. 2a](#)). The hydrothermal alteration may also affect the upper mafic crustal sequence of the ophiolitic sequences, which leads to the formation of epidote, chlorite and albite (e.g. [Alt et al., 1986](#); [Abd El-Rahman et al., 2009a, b](#)). Therefore, different band ratios were applied to detect the hydrothermal alteration at Logar valley area. The intimate association between chromite mineralization and serpentine in the Logar Valley area may make serpentinization a good indicator during mineral exploration and thus may provide useful information for discovering chromite deposits in other areas in Afghanistan. Four band ratios (R:6/7, G:4/2, B:5/4) (R:4/2, G:6/5, B:6/7) (R:4/2,G:6/7, B:10) and (R:4/2, G:6/7, B:5) were selected to detect the hydrothermal alteration for olivine and pyroxene that leads to the formation of serpentinized harzburgite at Logar Valley ([Fig. 5a, b, c, d](#)). The serpentinized ultramafic rocks of the Logar ophiolite are well-separated from the adjacent rock units in the band ratios (R:6/7, G:4/2, B:5/4) as a deep green-brown color ([Fig. 5a](#)). The serpentinized ultramafic rocks of the Logar ophiolite are poorly constrained with the other band ratios ([Fig. 5b, c, d](#)). The epidote-chlorite zone in the Logar ophiolite is identified by its red color in the band ratios (R:6/7, G:4/2, B:5/4) ([Fig. 5a](#)) and cyan color in the band ratios (R:4/2, G:6/5, B:6/7) ([Fig. 5b](#)); and high relief green spots in figures in the band ratios (R:4/2,G:6/7, B:10) and (R:4/2, G:6/7, B:5) ([Fig. 5c, d](#)).

A supervised classification based on Maximum Likelihood Classification (MLC) was performed for all previous band combinations to get better discrimination for the rock units. The training set was applied to calculate the variance and covariance to separate each rock units. Using MLC, the band combination R:7, G:5, B:2 ([Fig. 6a](#)), the serpentinized ultramafic rocks appear in green color, the Paghman metasedimentary rocks in blue color, the Khengil Series in cyan color to the north and south of the Logar ophiolite massif. The Neogene and Quaternary sediments occur in variable shades of yellow and recent valleys in melon red colors. The accuracy assessment was performed using old geological map and limited ground-truth data by a confusion matrix. The overall accuracy was almost 83% for MLC supervised classification method which is relatively high in overall accuracy.

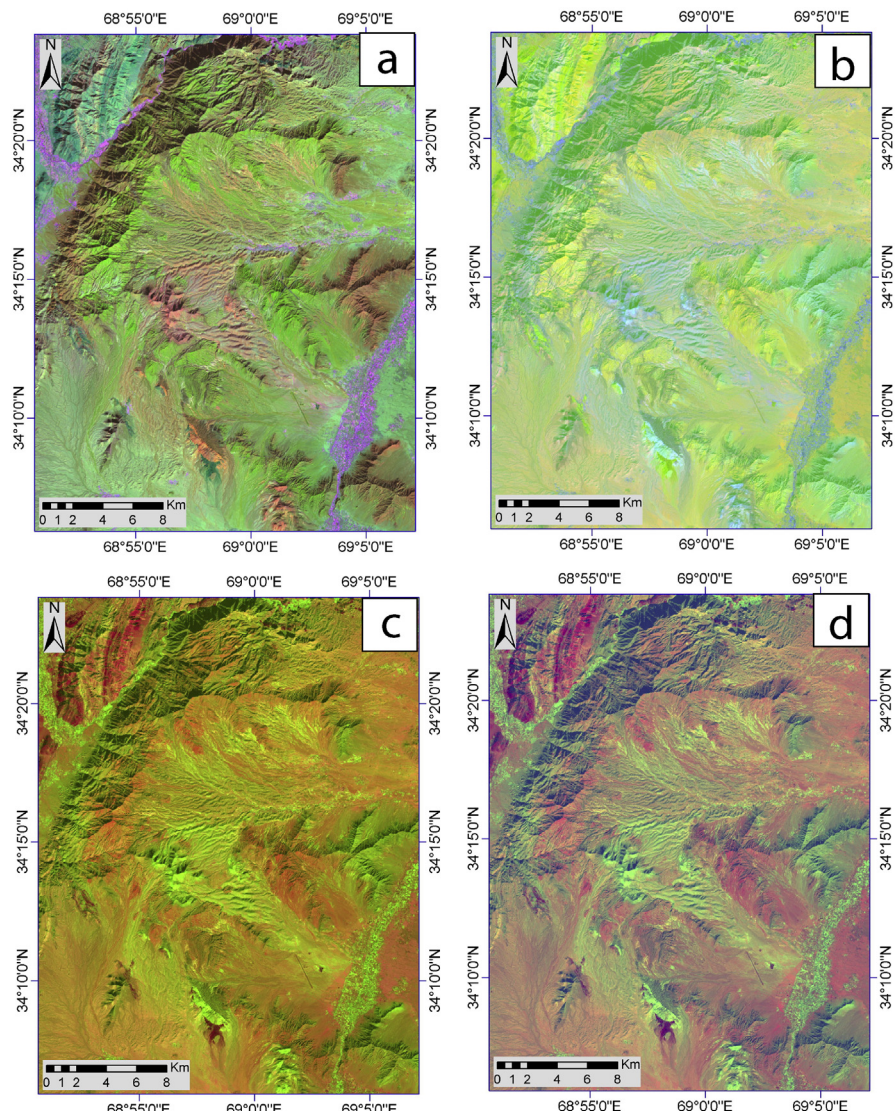


Fig. 5. Landsat8 OLI band ratio color image (A) (6/7, 4/2, 5/4), (B) (4/2, 6/5, 6/7), (C) (4/2, 6/7, 5), and (D) (4/2, 6/7, 10) in Logar Valley.

4. Discussion and conclusion

Remote sensing is widely used nowadays in lithological/geological mapping and in hydrothermal alteration detection, which is essential in distinguishing mineral deposits (Sabins, 1999). Recently, Landsat image has been implemented in a various applications, e.g. in the ecology (Salas et al., 2017), Environmental (Wang and Li, 2017), in water resources (Abdelaziz et al., 2008; Abdelaziz and Bakr, 2012; Abdelaziz and Merkel, 2012; Edet et al., 2014; Abdelaziz and Le, 2014; Abdelaziz and Bambi, 2016) geothermal resources (Qin et al., 2011; McNamara et al., 2016), mineral exploration (Mia and Fujimitsu, 2012), and Agriculture (Prishchepov et al., 2012). Many researchers around the world have used remote

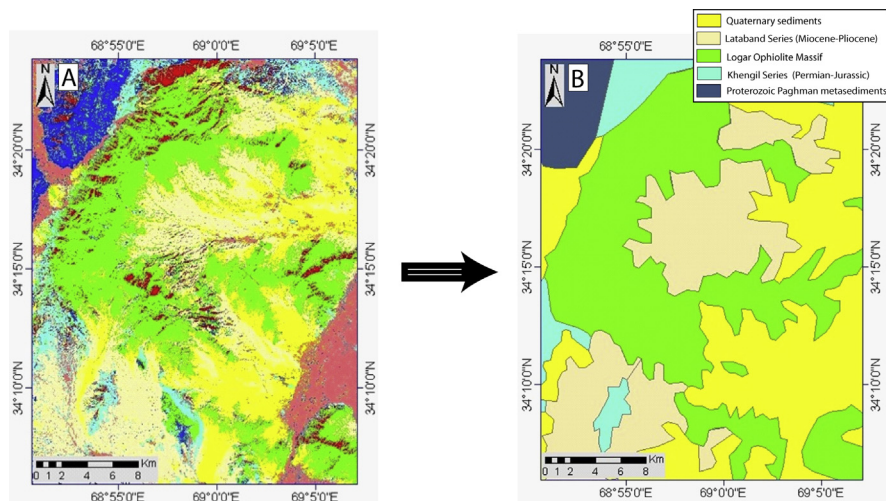


Fig. 6. (A) Supervised classified image for false color map (R7:G5:B2). (B) Geologic map of the Logar valley.

sensing data to differentiate serpentinized ultramafic rocks, which are hold potential for many types of deposits (e.g. Sultan et al., 1986; Gad and Kusky, 2006; Othman and Gloaguen, 2014, 2017; Pournamdar and Hashim, 2013; Azizi and Saibi, 2015; Rajendran and Nasir, 2014; Rajendran et al., 2013). Different methods and protocols are used in defining the serpentinized ultramafic rocks, such as ASTER (Tangestani et al., 2011; Rajendran and Nasir, 2014), Landsat TM (Sultan et al., 1986) and Landsat ETM+ (Gad and Kusky, 2006) satellite images. The previous studies had applied different image processing techniques like FCC (Pournamdar et al., 2014a, b), PCA (Qaoud, 2014), and band ratios (Sultan et al., 1986). Among these techniques, band ratios are the most common technique that are implemented to discriminate serpentinized ultramafic rocks using Landsat TM (5/7, 5/1, 5/4*3/4; Sultan et al., 1986), with Landsat ETM+ (5/3, 5/1, 7/5 and 7/5, 5/4, 3/1; Gad and Kusky, 2006), and with ASTER (4/7, 4/6, 4/10; Gad and Kusky, 2007) (4/7 and 4/7, 4/1, 2/3 and 4/3; Abdeen et al., 2001, and Rajendran and Nasir, 2014), (5/7, 5/4, 3/1; Mia and Fujimitsu, 2012), and (2 + 4/3, 5 + 7/6, 7 + 9/8; Amer et al., 2010). However, the previous band ratios are applicable for Landsat TM, ETM+, and ASTER. Different band ratios were studied for Landsat 8, it found that the most appropriate band ratios are (7/6, 6/5, 4/2), (6/4, 6/2, 7/6), and (6/7, 6/5, 4/2) with such as this arid region (Table 1).

Recently, The Logar Valley area was studied by remote sensing using PCA with multi-spectral ASTER imagery (Gale, 2011) and by Livo and Johnson (2011) using HyMap data from August 22 to October 2, 2007 to discriminate lithological units for the Logar Valley. Livo and Johnson (2011) processed HyMap data by Material Identification and Characterization Algorithm (MICA), which has limitation in differentiating the mineral with similar spectral range. It also has high cost and no public access. The Landsat

Table 1. A selected list of active sensors that used to separate the ophiolite.

Sensor	Launch Year	Band ratios	Reference
ASTER	1999	(4/7, 4/6, 4/10), (4/7, 3/4, 2/1), (4/7, 4/1, 2/3 * 4/3), and ((2 + 4)/3, (5 + 7)/6, (7 + 9)/8)	Gad and Kusky (2007), Abdeen et al. (2001), Rajendran and Nasir (2014), and Amer et al. (2010)
Landsat TM	1984	5/7, 5/1, 5/4*3/4	Sultan et al. (1986)
Landsat ETM+	2006	(5/3, 5/1, 7/5), (7/5, 5/4, 3/1), and (5/7, 5/4, 3/1)	Gad and Kusky (2006) and Mia and Fujimitsu (2012)
	2012		
Landsat-8	2013	(7/6, 6/5, 4/2), (6/4, 6/2, 7/6), and (6/7, 6/5, 4/2)	This study

8 has been adopted in this study instead of ASTER because the Landsat 8 has a higher end spectral range for TIR than ASTER (11.650 for ASTER and 12.50 for Landsat 8). Mapping serpentine requires higher spectral resolution; therefore Landsat 8 is the better sensor for this work. Additionally, Landsat 8 is easily accessible by the public and has a better coverage than ASTER. In contrast, ASTER can provide better spatial resolution (15 m for visible and 90 m for TIR ASTER), while Landsat can provide 30 m visible and 100 m TIR Landsat 8. Moreover, ASTER gives a better spectral resolution for NIR and TIR than Landsat 8. Using Landsat 8 as a tool for mineral exploration reduces the cost compared to the Imaging spectroscopy (HyMap). In this study, different techniques were used like FCC, PCA, and ratio images and among these, the most appropriate way of detection in such an arid region is the band ratios of (7/6, 6/5, 4/2), (6/4, 6/2, 7/6), and (6/7, 6/5, 4/2). These bands ratios give better discrimination for the rock units in the Logar Valley area and so a good delineation of the serpentized ultramafic rocks hosting the chromite in the area.

The results from all the image processing approaches is the map in Fig. 6b, which helps to classify the rock units of the Logar Valley area into five units. The first rocks unit is the Paghman metasedimentary rocks (dark blue color). The second unit is Khengil Series (cyan color) and the third category is Logar ophiolitic rocks (lawn green color). The low-relief areas are covered by the Neogene Lataband Series (beige color), and the Quaternary deposits (yellow color).

To conclude, the color composite ratio and the two band ration techniques (R:6/7, G:4/2, R:5/4) and (R:4/2, G:6/7, R:5) images with/without supervised classification give the best result for mapping the rock units and the alteration zones in the Logar Valley area. Thus, using supervised classification based on MLC provides a good tool to differentiate the different rock units in arid regions using Landsat 8. Clearly, the FCC technique shows a better distinction of the rock units in the Logar Valley area compared to the previous techniques. Moreover, the proposed methods can be

applied in different Provinces in the east and southeast of Afghanistan, like Kandahar, Khost, Nangarhar, Parvan, and Vardak Provinces, to detect the serpentinized ultramafic rocks, which are potential hosts for chromite and platinum group minerals.

Declarations

Author contribution statement

Ramadan Abdelaziz, Yasser Abd El-Rahman, Sophie Wilhelm: Conceived and designed the experiments; Performed the experiments; Analyzed and interpreted the data; Contributed reagents, materials, analysis tools or data; Wrote the paper.

Funding statement

This research did not receive any specific grant from funding agencies in the public, commercial, or not-for-profit sectors.

Competing interest statement

The authors declare no conflict of interest.

Additional information

No additional information is available for this paper.

Acknowledgements

The authors thank the associate editor whose constructive comments significantly improved the original manuscript. The authors thank Prof. Dr. Fayaz Saheb Jan for providing the chromite samples. I am grateful to Mrs. Autumn Dinkelman for help and support.

References

- Abd El-Rahman, Y., Polat, A., Dilek, Y., Fryer, B.J., El-Sharkawy, M., Sakran, S., 2009a. Geochemistry and tectonic evolution of the Neoproterozoic incipient arc-forearc crust in the Fawakhir area, Central Eastern Desert of Egypt. *Precambr. Res.* 175, 116–134.
- Abd El-Rahman, Y., Polat, A., Dilek, Y., Fryer, B.J., El-Sharkawy, M., Sakran, S., 2009b. Geochemistry and tectonic evolution of the Neoproterozoic Wadi Ghadir ophiolite, Eastern Desert, Egypt. *Lithos* 113, 158–178.

- Abdeen, M.M., Allison, T.K., Abdelsalam, M.G., Stern, R.J., 2001. Application of ASTER band-ratio images for geological mapping in arid regions; the Neoproterozoic Allaqa Suture, Egypt. *Abstr. Prog. Geol. Soc. Am.* 3, 289.
- Abdelaziz, R., Bakr, M.I., 2012. Inverse modeling of groundwater flow of Delta Wadi El-Arish. *J. Water Resour. Protect.* 4 (07), 432.
- Abdelaziz, R., Bambi, C.K.M., 2016. Groundwater assessment of the Bleone Catchment Karst aquifer in Southern France. *IOP Conf. Ser. Earth Environ. Sci.* 44 (2), 022028. IOP Publishing.
- Abdelaziz, R., Le, H.H., 2014. MT3DMSP – A parallelized version of the MT3DMS code. *J. Afr. Earth Sci.* 100, 1–6.
- Abdelaziz, R., Merkel, B.J., 2012. Analytical and numerical modeling of flow in a fractured gneiss aquifer. *J. Water Resour. Protect.* 4 (08), 657.
- Abdelaziz, R., Olsthoorn, T.N., Zhou, Y., Uhlenbrook, S., Smidt, E., 2008. Optimum Pumping-injection System for saline Groundwater Desalination in Sharm El Sheikh (No. 11, p. 21). Water Mill Working Paper.
- Abu El Ela, F.F., Farahat, E.S., 2010. Neoproterozoic podiform chromitites in serpentinites of the Abu Meriewa-Hagar Dungash district, Eastern Desert, Egypt: geotectonic implications and metamorphism. *Isl. Arc* 19, 151–164.
- Ahmed, A.H., 2013. Highly depleted harzburgite-dunite-chromitite complexes from the Neoproterozoic ophiolite, south Eastern Desert, Egypt: a possible recycled upper mantle lithosphere. *Precambrian Res.* 233, 173–192.
- Ahmed, A.H., Arai, S., Abdel-Aziz, Y.M., Ikenne, M., Rahimi, A., 2009. Platinum-group elements distributions and spinel composition in podiform chromitites and associated rocks from the upper mantle section of the Neoproterozoic Bou Azzer ophiolite, Anti-Atlas, Morocco. *J. Afr. Earth Sci.* 55, 92–104.
- Alt, J.C., Honnorez, J., Laverne, C., Emmerman, R., 1986. Hydrothermal alteration of a 1 Km section through the upper oceanic crust, Deep Sea Drilling Project Hole 504B: mineralogy, chemistry, and evolution of seawater-basalt interactions. *J. Geophys. Res.* 91, 309–335.
- Amer, R., Kusky, T., Ghulam, A., 2010. Lithological mapping in the Central Eastern Desert of Egypt using ASTER data. *J. Afr. Earth Sci.* 56, 75–82.
- Arai, S., 1997. Origin of podiform chromitite. *J. Asian Earth Sci.* 15, 303–310.
- Azizi, M., Saibi, H., 2015. Integrating gravity data with remotely sensed data for structural investigation of the Aynak-Logar Valley, Eastern Afghanistan, and the surrounding area. *IEEE J. Sel. Topics Appl. Earth Observ. Remote Sens.* 8 (2), 816–824.

- Benham, A.J., Kovac, P., Petterson, M.G., Rojkovic, I., Styles, M.T., Gunn, A.G., McKervey, J.A., Wasy, A., 2009. Chromite and PGE in the Logar Ophiolite Complex, Afghanistan. *Appl. Earth Sci. Trans. Inst. Min. Metall. B* 118, 45–58.
- Bohannon, R.G., 2010. Geologic and Topographic Maps of the Kabul South 30'x60', Afghanistan: U.S. Geological Survey Scientific Investigations Map 3137, 34p. Pamphlet, 2 Map Sheets, Scale 1:100,000 [Available at URL <http://pubs.usgs.gov/sim/3137>].
- Collet, S., Faryad, S.W., Mosazai, A.M., 2015. Polymetamorphic evolution of the granulite-facies Paleoproterozoic basement of the Kabul Block, Afghanistan. *Mineral. Petrol.* 109, 463–484.
- Dronov, V.I., Kalimulin, S.M., Sborshchikov, I.M., Svezhentsov, V.P., Chistyakov, A.N., Zelensky, E.D., Cherepov, P.G., 1972. The Geology and Minerals of North Afghanistan (Parts of Map Sheets 400-II and 500-I, the Kaysar-Hari Rod Interfluvia Area): [Afghanistan] Department of Geologic and Mineral Survey, 44p.
- Edet, A., Abdelaziz, R., Merkel, B., Okereke, C., Nganje, T., 2014. Numerical groundwater flow modeling of the coastal plain sand aquifer, Akwa Ibom State, SE Nigeria. *J. Water Resour. Protect.* 6 (04), 193.
- Faryad, S.W., Collett, S., Finger, F., Sergeev, S.A., Čopjaková, R., Simon, P., 2015. The Kabul Block (Afghanistan), a segment of the Columbia supercontinent, with a Neoproterozoic metamorphic overprint. *Gondwana Res.* 34, 221–240.
- Gad, S., Kusky, T.M., 2006. Lithological mapping in the Eastern Desert of Egypt, the Barramiya area, using Landsat thematic mapper (TM). *J. Afr. Earth Sci.* 44, 196–202.
- Gad, S., Kusky, T., 2007. ASTER spectral ratioing for lithological mapping in the Arabian–Nubian shield, the Neoproterozoic Wadi Kid area, Sinai, Egypt. *Gondwana Res.* 11 (3), 326–335.
- Gale, J., 2011. Ophiolite Mapping in Afghanistan a Case Study from the Logar Valley, GIS Poster Expo Gallery.
- González-Jiménez, J.M., Proenza, J.A., Gervilla, F., Melgarejo, J.C., Blanco-Moreno, J.A., Ruiz-Sánchez, R., Griffin, W.L., 2001. High-Cr and high-Al chromitites from Sagua de Tánamo district, Mayarí-Cristal ophiolitic massif (Eastern Cuba): constraints on their origin from mineralogy and geochemistry of chromian spinel and platinum group elements. *Lithos* 125, 101–121.
- Grieco, G., Merlini, A., 2012. Chromite alteration processes within Vaourinos ophiolite. *Int. J. Earth Sci.* 101, 1523–1533.

- Kafarsky, A. Kh., Chmyriov, V.M., Stazhilo-Alekseev, K.F., Abdullah, Sh., Saikovsky, V.S., 1975. Geological Map of Afghanistan, Scale 1:2,500,000.
- Livo, K.E., Johnson, M.R., 2011. Analysis of Imaging Spectrometer Data for the Aynak-Logar Valley Area of Interest. U.S. Geological Survey Open-File Report 2011-1204. Chapter 02B, pp. 95–134.
- McNamara, D.D., Bannister, S., Villamor, P., Sepúlveda, F., Milicich, S.D., Alcaraz, S., Massiot, C., 2016. Exploring structure and stress from depth to surface in the Wairakei Geothermal Field, New Zealand. In: Proc. 41st Stanford Workshop on Geothermal Reservoir Engineering, SGP-TR-209.
- Mia, B., Fujimitsu, Y., 2012. Mapping hydrothermal altered mineral deposits using Landsat 7 ETM+ image in and around Kuju volcano, Kyushu, Japan. *J. Earth Syst. Sci.* 121, 1049–1057.
- Miura, M., Arai, S., Ahmed, A.H., Mizukami, T., Okuno, M., Yamamoto, S., 2012. Podiformchromitite classification revisited: a comparison of discordant and concordant chromitite pods from Wadi Hilti, northern Oman ophiolite. *J. Asian Earth Sci.* 59, 52–61.
- Nevretdinov, E.B., Mirzamon, M., 1979. Report on Prospecting-survey and Evaluation Works on Asbestos, Chromite, and Other Raw Material in the Northern Part of the Logar Ultramafic Massif in 1978. Afghanistan Geological Survey Archive, Kabul.
- Orris, G.J., Bliss, J.D., 2002. Mines and mineral Occurrences of Afghanistan. U.S. Geological Survey Open-File Report 02-110, 95p.
- Othman, A.A., Gloaguen, R., 2014. Improving lithological mapping by SVM classification of spectral and morphological features: the discovery of a new chromite body in the Mawat Ophiolite Complex (Kurdistan, NE Iraq). *Rem. Sens.* 6 (8), 6867–6896.
- Othman, A.A., Gloaguen, R., 2017. Integration of spectral, spatial and morphometric data into lithological mapping: a comparison of different Machine Learning Algorithms in the Kurdistan Region, NE Iraq. *J. Asian Earth Sci.* 146, 90–102.
- Paktunc, A.D., 1990. Origin of podiform chromite deposits by multistage melting, melt segregation and magma mixing in the upper mantle. *Ore Geol. Rev.* 5, 211–222.
- Pournamdari, M., Hashim, M., 2013. Detection of chromite bearing mineralized zones in Abdash ophiolite complex using ASTER and ETM+ remote sensing data. *Arab. J. Geosci.* 7, 1973–1983.

- Pournamdari, M., Hashim, M., Pour, A.B., 2014a. Application of ASTER and Landsat TM data for geological mapping of Esfandagheh ophiolite complex, southern Iran. *Resour. Geol.* 64, 233–246.
- Pournamdari, M., Hashim, M., Pour, A.B., 2014b. Spectral transformation of ASTER and Landsat TM bands for lithological mapping of Soghan ophiolite complex, south Iran. *Adv. Space Res.* 54, 694–709.
- Prishchepov, A.V., Radeloff, V.C., Dubinin, M., Alcantara, C., 2012. The effect of Landsat ETM/ETM+ image acquisition dates on the detection of agricultural land abandonment in Eastern Europe. *Rem. Sen. Environ.* 126, 195–209.
- Qaoud, N., 2014. Utilization of space-borne imagery for lithologic mapping: a case study from Um Had Area, Central Eastern Desert, Egypt. *J. Geogr. Geol.* 6, 113–123.
- Qin, Q., Zhang, N., Nan, P., Chai, L., 2011. Geothermal area detection using Landsat ETM+ thermal infrared data and its mechanistic analysis—a case study in Tengchong, China. *Int. J. Appl. Earth Obs. Geoinf.* 13 (4), 552–559.
- Rajendran, S., Nasir, S., 2014. Hydrothermal altered serpentized zone and a study of Ni-magnesioferrite–magnetite–awaruite occurrences in Wadi Hibi, Northern Oman Mountain: discrimination through ASTER mapping. *Ore Geol. Rev.* 62, 211–226.
- Rajendran, S., al-Khirbashi, A., Pracejus, B., Nasir, S., Al-Abri, A.H., Kusky, T.M., Ghulam, A., 2012. ASTER detection of chromite bearing mineralized zones in Semail Ophiolite Massifs of the northern Oman Mountains: exploration Strategy. *Ore Geol. Rev.* 44, 121–135.
- Rajendran, S., Nasir, S., Kusky, T.M., Ghulam, A., Gabr, S., El-Ghali, M.A., 2013. Detection of hydrothermal mineralized zones associated with listwaenites in Central Oman using ASTER data. *Ore Geol. Rev.* 53, 470–488.
- Rollinson, H., 2005. Chromite in the mantle section of the Oman ophiolite: a new genetic model. *Isl. Arc* 14, 542–550.
- Sabins, F.F., 1999. Remote sensing for mineral exploration. *Ore Geol. Rev.* 14, 157–183.
- Salas, E.A.L., Valdez, R., Michel, S., 2017. Summer and winter habitat suitability of Marco Polo argali in southeastern Tajikistan: a modeling approach. *Heliyon* 3 (11), e00445.
- Shahtahmassebi, A., Yang, N., Wang, K., Moore, N., Shen, Z., 2013. Review of shadow detection and de-shadowing methods in remote sensing. *Chin. Geogr. Sci.* 23, 403–420.

- Shareq, A., Voinov, V.N., Nevretdinov, E.B., Kubatkin, L.V., Gusav, I.A., 1980. The Logar ultrabasite massif and its reflection in the magnetic field (East Afghanistan). *Tectonophysics* 62, 1–5.
- Sultan, M., Arvidson, R.E., Sturchio, N.C., 1986. Mapping of serpentinites in the Eastern Desert of Egypt by using landast thematic mapper data. *Geology* 14, 995–999.
- Tangestani, M.H., Jaffari, L., Vincent, R.V., Sridhar, B.B.M., 2011. Spectral characterization and ASTER-based lithological mapping of an ophiolite complex: a case study from Neyriz ophiolite, SW Iran. *Rem. Sen. Environ.* 115, 2243–2254.
- Tapponnier, P., Mattauer, M., Proust, F., Cassaigneau, C., 1981. Mesozoic sutures, and large-scale tectonic movements in Afghanistan. *Earth Planet Sci. Lett.* 52, 355–371.
- Volin, W., 1974. The Chromite Deposits in the Logar Valley in Kabul Province, Afghanistan. Unpublished report in Afghanistan Geological Survey Archive.
- Wang, Z.H., Li, Q., 2017. Thermodynamic characterisation of urban nocturnal cooling. *Heliyon* 3 (4), e00290.